Direct Physical Exfoliation of Few-Layer Graphene from Graphite Grown on a Nickel Foil Using Polydimethylsiloxane (PDMS) with Tunable Elasticity and Adhesion

Kwanghyun Yoo[1], Yusuke Takei[1], Sungjin Kim[2], Shohei Chiashi[2], Shigeo Maruyama[2], Kiyoshi Matsumoto[3] and Isao Shimoyama[1,3]

[1]Department of Mechano-Informatics, Graduate School of Information Science and Technology, The University of Tokyo, 7-3-1 Hongo, Bunkyo-ku, Tokyo, 113-8656, Japan

[2]Department of Mechanical Engineering, School of Engineering, The University of Tokyo, 7-3-1 Hongo, Bunkyo-ku, Tokyo, 113-8656, Japan

[3]Information and Robot Technology Research Initiative, The University of Tokyo, 7-3-1 Hongo, Bunkyo-ku, Tokyo, 113-8656, Japan

Short title: Direct Physical graphene exfoliation from graphite using optimized PDMS

PACS codes: 68.65.Pq, 81.05.ue, 81.05.uf, 81.07.-b, 82.35.Gh, 82.35.Lr, 83.80.Va, 61.25.hp

Corresponding author

Tel: +81-3-5841-0461

Fax: +81-3-5841-0835

Isao Shimoyama: isao@leopard.t.u-tokyo.ac.jp

ABSTRACT

We firstly introduce a facile method for the site-specific direct physical exfoliation of few-layer graphene sheets from cheap and easily enlargeable graphite grown on a Ni foil using an optimized polydimethylsiloxane (PDMS) stamp. By decreasing the PDMS cross-linking time, the PDMS elasticity is reduced to ~52 kPa, similar to that of a typical gel. As a result of this process, the PDMS becomes more flexible yet remains in a handleable state as a stamp. Furthermore, the PDMS adhesion to a graphite/Ni surface, as measured by the peel strength, increases to ~5.1 N/m, which is approximately 17 times greater than that of typical PDMS. These optimized properties allow the PDMS stamp to have improved contact with the graphite/Ni surface, including the graphite wrinkles. This process is verified, and changes in surface morphology are observed using a 3D laser scanning microscope. Under conformal contact, the optimized PDMS stamp demonstrates the site-specific direct physical exfoliation of few-layer graphene sheets including mono- and bi-layer graphene sheets from the graphite/Ni substrate without the use of special equipment, conditions or chemicals. The number of layers of the exfoliated graphene and its high quality are revealed by the measured Raman spectra. The exfoliation method using tunable elasticity and adhesion of the PDMS stamp can be used not only for cost effective mass production of defect-less few-layer graphene from the graphite substrate for micro/nano device arrays but also for nano-contact printing of various structures, devices and cells.

1. Introduction

Graphene, a two-dimensional layer of carbon atoms arranged in a hexagonal lattice, was first isolated in 2004 [1]. Since then, graphene has attracted considerable attention due to its high electron mobility [1], mechanical strength [2], thermal conductivity [3], light transmittance [4] and easily modified electrical properties by electric and magnetic fields [5]. Because of the potential to resolve scientific problems and improve device performance, complementary methods for suitable graphene fabrication have been competitively introduced, such as chemical exfoliation of graphite oxide [6], epitaxial growth on a silicon carbide substrate [7] and chemical vapor deposition (CVD) with a metal catalyst [8].

Compared with these fabrication processes, a physical exfoliation method is a straightforward route because it directly peels graphene from bulk graphite under dry condition using only a stamp and without the use of a special apparatus or materials [1]. Moreover, this method does not involve mechanical damage to the graphene because the extreme anisotropy between the shear modulus of graphite interlayer (~0.48 MPa [9]) and the elastic modulus in the graphene basal plane (~1TPa [2]) allow the graphene to retain its intrinsic crystal structure during physical separation [10]. Therefore, this method is considered a suitable approach for the simple yet defect-less fabrication of micro/nano scale arrays of few-layer (e.g., less than 10 layers) graphene sheets.

Since 2004, Scotch tape has been used to exfoliate graphene from highly ordered pyrolytic graphite (HOPG) for scientific investigations into intrinsic graphene or feasibility studies of graphene-based devices [1]. However, repeating the exfoliation process is inherently required to reduce the number of layers of graphene from multi-layers down to mono- or few-layers because the use of un-scalable tape causes random exfoliations.

Instead of tape, Li *et al* employed a silicon dioxide (SiO_2) stamp and applied high pressures to the HOPG underneath the SiO_2 to induce graphite interlayer separation [11]. However, instead of few-layer graphene sheets, this process directly exfoliated multi-layer graphene sheets of 5.8-71 nm thick, which corresponds to between several tens to hundreds of layers. The high thickness fluctuation is attributed to the application of high pressure and poor contact between the rigid SiO_2 stamp and the HOPG surfaces.

To improve contact between the stamp and the graphite, a gold (Au) film was deposited onto the HOPG surface. This process produced a set of directly exfoliated few-layer graphene less than 10 layers [12]. A palladium (Pd) film has also been employed for this purpose [13]. However, the use of metal films introduces chemical problems

resulting from metal etching required for transferring the exfoliated graphene to a substrate (e.g., SiO_2/Si) [14]. Indeed, after the Pd film underneath the graphene was etched with an HCl/$FeCl_3$-based etchant, Pd and Fe atoms were found on the exfoliated graphene surface [13], which can cause un-wanted doping and chemical damage.

In contrast to these metal films, a PDMS stamp after the graphene exfoliation process not only can be removed from the exfoliated graphene sheets without quality degradation from the chemical etching process but also can directly be used as a substrate of the exfoliated graphene sheet for transparent and stretchable device applications [15]. Despite these advantages, the use of the PDMS stamp is limited by the non-conformal contact with the graphite surface, resulting in the un-site-specific and random exfoliation of few-layer graphene sheets [16]. Therefore, properties of the typical PDMS stamp, especially the adhesion property, should be enhanced to make conformal contact with the graphite surface. Moreover, alternative graphite substrate should be employed to realize potential mass production of arrays of damage-less few-layer graphene sheets because the exfoliated graphene area is limited by the use of conventional HOPG (10×10 mm^2), which is not easily scaled up.

Here we firstly propose a site-specific direct physical exfoliation method for few-layer graphene sheets from a CVD-graphite/Ni surface using an optimized PDMS stamp without the use of special equipment, conditions or chemicals (see figure 1). In this method, rather than using conventional HOPG, a relatively cheap and easily enlargeable CVD-graphite/Ni surface is used as a precursor for graphene to examine potential low cost batch fabrication of few-layer graphene arrays. The CVD-graphite can easily be pattered by typical lithographic technique for the direct exfoliation of the pre-defined graphene sheets (e.g., FET channel with contact pads). In addition, instead of the typical PDMS stamp, an optimized PDMS stamp having the enhanced adhesion to the graphite surface is used because it can improve contact with the graphite/Ni surface, even a few nanometers graphite wrinkles. Finally, we demonstrate the site-specific direct physical exfoliation of defect-less few-layer graphene sheets from the CVD-graphite/Ni surface using the optimized PDMS stamp.

2. Graphite grown on a Ni foil by alcohol catalytic CVD (ACCVD)

The graphite/Ni sample is prepared via alcohol catalytic chemical vapor deposition (ACCVD). This method has several advantages. Alcohol is a cheaper and more stable carbon source than the more typically used methane gas

(CH_4), which is relatively expensive and potentially explosive under the growth process conditions, including temperatures of approximately 1000°C [8, 17]. Furthermore, unlike CH_4, the etching effect of the hydroxyl group (-OH) decomposed from the alcohol molecule (C_2H_5OH) suppresses the formation of impurities, such as amorphous carbon [18]. Therefore, using alcohol facilitates the growth of high-purity graphite and graphene [17] as well as single-walled carbon nanotubes [18].

A polycrystalline Ni foil (50 μm thick, 99% purity, Nilaco Co.) was used as a catalyst to grow graphite because of its high carbon solubility [17]. The Ni foil inside the ACCVD chamber was heated to 1000°C for 10 min with an Ar/H_2 gas flow of 300 standard cubic centimeters per minute (sccm) to promote grain enlargement [19]. The alcohol vapor carbon source was introduced into the chamber for 10 min. Afterwards, the Ni foil was immediately cooled to room temperature at an average rate of ~3.25 °C/sec under Ar/H_2 gas flow so that graphite formed on the Ni surface.

Figure 2 shows the characteristics of the graphite/Ni sample grown via ACCVD. The Raman spectrum of the graphite/Ni sample was taken with a resonance Raman spectrometer (Chromex 501is spectrometer and an Andor DV401-FI CCD system) using a 488 nm wavelength laser as the excitation source, as shown in figure 2(a). The presence of graphite (also called multi-layer graphene) is confirmed by the relatively strong and sharp G peak at approximately 1580 cm^{-1} in the bottom Raman spectrum compared to that of the mono-layer graphene reference [20]. The Raman spectrum of the graphite/Ni exhibits small, split 2D peaks where the primary peak should be (at ~2721 cm^{-1}) and a secondary peak at ~2682 cm^{-1}. These peaks originate from the splitting of the electronic band structure in the multi-layered graphene [21]. These characteristics and the negligible D peak at ~1350 cm^{-1} verify the growth of high quality graphite/Ni because the peaks tend to increase with increasing amounts of crystal disorder or contaminants, reflecting the crystal quality and purity associated with graphene [22]. The image from the scanning electron microscope (see figure 2(a), inset) shows graphite wrinkles that originate from the thermal expansion coefficient difference between the graphite and the nickel [8]. The intimate morphology of the graphite/Ni surface was observed by a 3D laser scanning microscope (VK-9710, Keyence Co.), as shown in figure 2(b). Figure 2(c) shows the surface morphology magnified in the area highlighted by the dashed line. Valley-like Ni grain boundaries (denoted by red arrows) and ridge-like graphite wrinkles (denoted by blue arrows) are seen on the graphite/Ni surface (figure 2(c)) and are described in the schematic illustration of the graphite/Ni cross-section (figure 2(d)).

3. Tuning elasticity and adhesion of PDMS

The elasticity and adhesion of the PDMS were adjusted by varying the PDMS cross-linking time to determine an optimal PDMS stamp for the direct physical exfoliation of graphene under conformal contact. A thermally curable PDMS monomer and a curing agent (KE-106 and CAT-RG, Shin-Etsu Chemical Co.) were mixed to a 10:1 weight ratio, and fabricated into PDMS stamps using the parameters summarized in Table 1. After centrifugal mixing at 2000 rpm for 40 sec and defoaming at 2000 rpm for 20 sec using a conditioning mixer (ARE-250, Thinky Co.), 5 grams of the mixture was poured into six Petri dishes (4 inch diameter). These samples were degassed in a vacuum desiccator at -80 kPa (i.e., gauge pressure) for 20 min. After degassing, the samples were cross-linked for between 20-120 min at the fixed temperature of 70°C because the cross-linking density of the PDMS networks is affected by the interplay between the cross-linking time and the temperature [23]. Immediately after cross-linking, the samples were cooled to below room temperature in a refrigerator to quickly remove any residual thermal energy that might cause unwanted additional cross-linking in the samples.

3.1. Elasticity of PDMS

Compression tests were performed to quantitatively evaluate the elastic moduli of the PDMS samples against the cross-linking time. Different PDMS samples cross-linked for 20-120 min were cut into $5 \times 5 \times 4.5$ mm^3 blocks (length × width × thickness). A 5% compressive strain was applied to each of the PDMS samples, and the applied force was measured six times using a force gauge attached to a motorized stage (ZPS-DPU 50N, Imada).

Figure 3 shows the elastic modulus and flexibility of the PDMS versus the cross-linking time. The average elastic moduli and the standard deviations versus the PDMS cross-linking time are obtained from the six measurements, as plotted in figure 3(a). Additionally, the relationship between the cross-linking time, the elastic moduli and the PDMS characteristics (i.e., state and handleability) are summarized in Table 2. The elastic modulus tends to decrease with decreasing cross-linking time, and a rapid decrease is observed for cross-linking times less than 40 min. The PDMS sample cross-linked for 60 min shows an elastic modulus of ~1.48 MPa, which agrees well

with typical PDMS characteristics [24, 25]. When the PDMS cross-linking time is reduced from 60 min to 20 min, the PDMS reverts to a sticky gel-like state that cannot be handled as a stamp (Table 2). By contrast, the PDMS sample with a cross-linking time of 25 min exhibits moderate durability and a low elastic modulus of ~52 kPa, which is two orders of magnitude smaller than that of typical PDMS (cross-linked for 60 min) and is similar to that of a normal gel [26]. Figure 3(b) shows photographs of cantilevers made from different PDMS samples cross-linked for 20-60 min. Deflections in the PDMS cantilevers under gravity show that flexibility is enhanced as the PDMS cross-linking time is decreased. Although the most flexible PDMS sample (cross-linked for 20 min) can suppress the elastic recovery that impedes conformal contact with a rough surface, it cannot be handed as a stamp. However, the PDMS sample that was cross-linked for 25 min offers moderate handleability as a stamp, as well as relatively high flexibility compared with the samples that were cross-linked for 30-120 min. For these reasons, the PDMS sample cross-linked for 25 min is considered the optimal stamp to provide improved contact with the rough graphite/Ni surface for direct physical graphene exfoliation.

3.2. Adhesion of PDMS

A peel test was conducted to examine the adhesion between the PDMS and the graphite/Ni surfaces as a function of the cross-linking time. The 90° peel strength (defined force per unit width: N/m) between the 20 mm wide PDMS and the graphite surfaces was measured five times using a force gauge. The results are summarized in the inset table in figure 4(a). The peel strength increases with decreasing PDMS cross-linking time (figure 4(a)), which is the opposite trend seen for the elastic modulus (figure 3(a)). This trend shows that flexibility as a result of reduced elasticity enhances the adhesion of the PDMS to the graphite surface. The PDMS sample cross-linked for 25 min has a peel strength of ~5.1 N/m, which is ~17 times greater than that typically seen for PDMS cross-linked for 60 min (~0.3 N/m). Additionally, the peel strength is one order of magnitude greater than the graphite interlayer bonding [9]. Therefore, the PDMS sample cross-linked for 25 min is determined to be the optimal stamp, providing enhanced adhesion and moderate handleability when compared to other PDMS stamp samples (see Table 2).

To examine the contact characteristics of the optimized PDMS stamp, the post-debonding surface morphology of the graphite/Ni surface was observed with an optical microscope. Patterns that are imprinted from the rough graphite/Ni surface are seen on the PDMS sample cross-linked for 25 min (denoted by white arrows in figure 4(b)),

whereas the surface of PDMS sample cross-linked for 60 min does not show any imprinting (see figure 4(c)). These patterns show that the optimized properties of PDMS samples cross-linked for 25 min play a significant role in improving the contact properties with the rough graphite/Ni surface.

The detailed morphology of the debonded surface of the PDMS sample cross-linked for 25 min from the graphite/Ni substrate was observed using the 3D laser scanning microscope, as shown in figure 5(a). Figure 5(b) shows the magnified surface morphology of the area highlighted with a dashed line. Figure 5(c) shows a schematic illustration of the cross-section of the graphene/PDMS. Ridge-like patterns (denoted by red arrows) were confirmed to exist on the PDMS surface (figure 5(b)), which are the corresponding structures matching the Ni grain boundaries (figure 2(c)). Valley-like patterns (denoted by blue arrows) were also found imprinted on the PDMS surface from the graphite wrinkles (Figure 5(b)). The changes in the surface morphology demonstrate that the optimized PDMS stamp makes conformal contact with not only the grain boundaries of the Ni foil underneath the graphite but also the graphite wrinkles (known to be a few nanometers tall [27]), which is highly desired for direct physical exfoliation of graphene sheets.

4. Direct physical exfoliation of few-layer graphene from CVD-graphite/Ni

The direct physical exfoliation method for the creation of few-layer graphene sheets is demonstrated using a pre-patterned CVD-graphite/Ni sample with the optimized PDMS stamp. An aluminum (Al) layer (~300 nm thick) as an etch mask was deposited on the graphite/Ni surface via a shadow mask. An array of graphite patterns (~400 × 400 μm^2) was then defined by oxygen plasma etching for site specific direct exfoliation of the graphene sheets, as shown in figure 6(a). The surface of the square patterned graphite was scanned by an atomic force microscopy (AFM, L-Trace II with Nanonavi Station, SII Nanotechnology Inc.). Figure 6(b) shows the AFM image of the graphite surface across the bare Ni surface etched by oxygen plasma. The AFM image reveals that the thickness of the patterned graphite is ~271 nm which corresponds to approximately 800 layers graphene sheets because a graphene sheet has ~0.34 nm [8]. In addition, it is confirmed that the side wall of the graphite edge has ~189 nm in thickness (i.e., ΔZ of B) and ~769 nm in width (i.e., distance between B_Z1 and B_Z2), as shown in the inset table in figure 6(b).

To directly and physically exfoliate few-layer graphene sheets, when the optimal PDMS stamp was bonded with the pre-patterned graphite/Ni sample for 60 min, they were pressed at 10 N for 5 min using the force gauge. While debonding the PDMS stamp the graphite/Ni surface, few-layer graphene sheets were exfoliated onto the surface of the PDMS stamp. Figure 6(c) shows a microscope image of an array of exfoliated graphene on the PDMS surface (highlighted by white brackets).

To characterize the exfoliated graphene, Raman spectra were obtained from different graphene patterns exfoliated on the PDMS surfaces by a resonance Raman spectrometer (excited by a 488 nm wavelength laser), as shown in figure 7(a). The intensity ratio between the 2D and G peaks (I_{2D}/I_G) and the full width at half maximum (FWHM) value of the 2D band in the Raman spectrum allow the determination of the number of exfoliated graphene sheets [20-22]. The formation of mono-layer graphene is verified from the highest I_{2D}/I_G ratio (i.e., ~4) and the narrowest FWHM value from the 2D peak (i.e., ~30) in the topmost Raman spectrum (i.e., black line), as shown in figure 7(a). Additionally, when compared to mono-layer graphene, the relatively low I_{2D}/I_G ratio and the wide FWHM value of the 2D peak in the two intermediate Raman spectra (i.e., red and blue lines) indicate the existence bi- and few-layer graphene [21, 22, 28]. The negligible D peak at ~1350 cm^{-1} in the Raman spectra represents defect-less, high quality exfoliated graphene sheets [22]. Moreover, the unusual peak at ~1410 cm^{-1} (denoted by an arrow and asterisk) is a characteristic footprint of the PDMS arising from the asymmetric CH_3 bend [21, 22, 28], as shown in the bottom Raman spectrum (i.e., pink line) of the bare PDMS.

Scanning micro-Raman of the graphene sheets exfoliated on the PDMS surface was conducted with a micro-Raman spectroscopy (Raman-11 system, Nanophoton Co., Ltd.) in order to evaluate the uniformity of the exfoliated graphene sheets. Figure 7(b) shows the scanning Raman map of I_{2D}/I_G of the exfoliated graphene sheets taken from a 20 × 20 μm^2 area. In the Raman map, I_{2D}/I_G decrease with increasing the number of graphene layers. The result of Raman mapping reveals the uniformity of the exfoliated graphene sheets which are mostly few-layer graphene sheets, showing I_{2D}/I_G around 1. The exfoliated graphene near the graphite edge (top side in the figure 7(b)) shows relatively high thickness variation, compared to the exfoliated graphene relatively far from the graphite edge (bottom side in the figure 7(b)). After the graphene exfoliation process, the PDMS stamp underneath the exfoliated graphene sheets can be used as a substrate for graphene-based transparent and stretchable device applications, without the need of transferring the exfoliated graphene sheets onto other substrate.

From these experiments, we demonstrated that the proposed direct physical exfoliation method can produce few-layer graphene including mono- and bi-layer graphene, although not uniform mono-layer graphene. This simple and low cost fabrication method can be used for arrays of micro/nano devices using the few-layer graphene sheets.

The screening effect from the conformal contact between the PDMS/graphite weakens the graphite interlayer bonding near the PDMS/graphite interface, whereas other interlayers that are farther away from the PDMS/graphite interface remain initially bonded because the van der Waals interactions significantly decrease with increasing mutual distance [11, 29]. Consequently, neighboring mono- or few-layer graphene sheets can be preferentially exfoliated from the graphite under conformal contact. Therefore, to realize potential uniform exfoliation of mono-layer graphene which is governed by the screening effect, it is essential not only to prepare the uniform and defect/vacancy-free graphite substrate as a graphene precursor but also to optimize contact between the stamp and graphite surfaces.

Conclusions

We have firstly demonstrated the site-specific direct physical exfoliation of defect-less few-layer graphene sheets from a CVD-graphite/Ni surface using an optimized PDMS stamp. Highly flexible, adhesive yet handleable PDMS cross-linked for 25 min was found to be the optimal stamp material to make conformal contact over the entire graphite/Ni surface, including the nano-scale graphite wrinkles. The stamp permitted direct physical exfoliation of defect-less few-layer graphene including mono- and bi-layer graphene from the graphite/Ni surface without the use of special equipment, conditions or chemicals. The proposed graphene exfoliation method using cost-effective and easily scalable CVD-graphite can be employed for the potential low-cost mass production of arrays of micro/nano scale sheets of few-layer graphene for different device applications. In addition, the facile yet quantitative tuning method to adjust the PDMS properties can be applied to prepare an optimal stamp not only for graphene exfoliation but also for nano-contact printing of various structures, devices and cells.

Acknowledgement

This work is partly supported by "Iketani Science and Technology Foundation" and "Mizuho Foundation for the Promotion of Sciences".

REFERENCES

[1] Novoselov K S, Geim A K, Morozov S V, Jiang D, Zhang Y, Dubonos S V, Grigorieva I V and Firsov A A 2004 Electric Field Effect in Atomically Thin Carbon Films *Science* **306** 666-669

[2] Lee C, Wei X, Kysar J W and Hone J 2008 Measurement of the Elastic Properties and Intrinsic Strength of Monolayer Graphene *Science* **321** 385-388

[3] Balandin A A, Ghosh S, Bao W, Calizo I, Teweldebrhan D, Miao F and Lau C N 2008 Superior Thermal Conductivity of Single-Layer Graphene *Nano Lett.* **8** 902-907

[4] Nair R R, Blake P, Grigorenko A N, Novoselov K S, Booth T J, Stauber T, Peres N M R and Geim A K 2008 Fine Structure Constant Defines Visual Transparency of Graphene *Science* **320** 1380

[5] Neto A H, Guinea F, Peres N M R, Novoselov K S and Geim A K 2009 The electronic properties of graphene *Rev. Mod. Phys.***81** 109-162

[6] Stankovich S, Piner R D, Chen X, Wu N, Nguyen S T and Ruoff S R 2006 Stable aqueous dispersions of graphitic nanoplatelets via the reduction of exfoliated graphite oxide in the presence of poly(sodium 4-styrenesulfonate) *J. Mater. Chem.* **16** 155-158

[7] Berger C, Song Z, Li X, Wu X, Brown N, Naud C, Mayou D, Li T, Hass J, Marchenkov A N, Conrad E H, First P N and de Heer W A 2006 Electronic Confinement and Coherence in Patterned Epitaxial Graphene *Science* **312** 1191-1196

[8] Kim K S, Zhao Y, Jang H, Lee S Y, Kim J M, Kim K S, Ahn J H, Kim P, Choi J Y and Hong B H 2009 Large-scale pattern growth of graphene films for stretchable transparent electrodes *Nature* **457** 706-710

[9] Soule D E and Nezbeda C W 1968 Direct Basal Plane Shear in Single Crystal Graphite *J. Appl. Phys.* **39** 5112-5139

[10] Geim A K 2009 Graphene: Status and Prospects *Science* **324** 1530-1534

[11] Li D, Windl W and Padture N P 2009 Toward Site-Specific Stamping of Graphene *Adv. Mater.* **21** 1243-1246

[12] Song L, Ci L, Gao W and Ajayan P M 2009 Transfer Printing of Graphene Using Gold Film *ACS Nano* **3** 1353-1356

[13] Unarunotai S, Koepke J C, Tsai C L, Du F, Chialvo C E, Murata Y, Haasch R, Petrov I, Mason N, Shim M Lyding J and Rogers J A 2010 Layer-by-Layer Transfer of Multiple, Large Area Sheets of Graphene Grown in Multilayer Stacks on a Single SiC Wafer *ACS Nano* **4** 5591-5598

[14] Yoo K, Takei Y, Hou B, Chiashi S, Maruyama S, Matsumoto K and Shimoyama I 2011 Direct Physical Exfoliation and Transfer of Graphene Grown via Ethanol Chemical Vapor Deposition *Proc. IEEE Int. Conf. on Micro Electro Mechanical Systems* 99-102

[15] Lee Y, Bae S, Jang H, Jang S, Zhu S E, Sim S H, Song Y I, Hong B H and Ahn J H 2010 Wafer-Scale Synthesis and Transfer of Graphene Films *Nano Lett.* **10** 490-493

[16] Goler S, Piazza V, Roddaro S, Pellegrini V, Beltram F and Pingue P 2011 Self-assembly and electron-beam-induced direct etching of suspended graphene nanostructures *J. Appl. Phys.***110** 064308

[17] Miyata Y, Kamon K, Ohashi K, Kitaura R, Yoshimura M and Shinohara H 2010 A simple alcohol-chemical vapor deposition synthesis of single-layer graphenes using flash cooling *Appl. Phys. Lett.* **96** 263105

[18] Maruyama S, Kojima R, Miyauchi Y, Chiashi S and Kohno M 2002 Low-temperature synthesis of high-purity single-walled carbon nanotubes from alcohol *Chem. Phys. Lett.* **360** 229-234

[19] Thiele S, Reina A, Healey P, Kedzierski J, Wyatt P, Hsu P L, Keast C, Schaefer J and Kong J 2010 Engineering polycrystalline Ni films to improve thickness uniformity of the chemical-vapor-deposition-grown graphene films *Nanotechnology* **21** 015601

[20] Graf D, Molitor F, Ensslin K, Stampfer C, Jungen A, Hierold C and Wirtz L 2007 Spatially Resolved Raman Spectroscopy of Single- and Few-Layer Graphene *Nano Lett.* **7** 238-242

[21] Ni Z, Wang Y, Yu T and Shen Z 2008 Raman Spectroscopy and Imaging of Graphene *Nano Res.* **7** 273-291

[22] Ferrari A C, Meyer J C, Scardaci V, Casiraghi C, Lazzeri M, Mauri F, Piscanec S, Jiang D, Novoselov K S, Roth S and Geim A K 2006 Raman Spectrum of Graphene and Graphene Layers *Phys. Rev. Lett.* **97** 187401

[23] Fuard D, Chevolleau T, Decossas S, Tracqui P and Schiavone P 2008 Optimization of poly-di-methyl-siloxane (PDMS) substrates for studying cellular adhesion and motility *Microelectronic Eng.* **85** 1289-1293

[24] Hocheng H, Chen C M, Chou Y C and Lin C H 2010 Study of novel electrical routing and integrated packaging on bio-compatible flexible substrates *Microsyst. Technol.* **16** 423-430

[25] Rafat M, Raad D R, Rowata A C and Auguste D T 2008 Fabrication of reversibly adhesive fluidic devices

using magnetism *Lab Chip* **9** 3016-3019

[26] Jacot J G, McCulloch A D and Omens J H 2008 Substrate Stiffness Affects the Functional Maturation of Neonatal Rat Ventricular Myocytes *Biophys. J.* **95** 3479-3487

[27] Chae S J, Gunes F, Kim K K, Kim E S, Han G H, Kim S M, Shin H J, Yoon S M, Choi J Y, Park M H, Yang C W, Pribat D and Lee Y H 2009 Synthesis of Large-Area Graphene Layers on Poly-Nickel Substrate by Chemical Vapor Deposition: Wrinkle Formation *Adv. Mater.***21** 2328-2333

[28] Pryce Lewis H G, Casserly T B and Gleason K K 2001 Hot-Filament Chemical Vapor Deposition of Organosilicon Thin Films from Hexamethylcyclotrisiloxane and Octamethylcyclotetrasiloxane *J. Electrochem. Soc.* **148** 212-220

[29] Sabio J, Seoánez C, Fratini S, Guinea F, Castro Neto A H and Sols F 2008 Electrostatic interactions between graphene layers and their environment *Phys. Rev. B* **77** 195409

List of captions of Tables

Table 1 Parameters for the fabrication of the PDMS samples.

Table 2 Summary of the elastic moduli and characteristics of the PDMS samples versus the cross-linking time. The average (Avg.) values and standard deviations (S.D.) were calculated from six different measurements.

List of captions of Figures

Figure 1 Schematic illustration of the direct physical exfoliation of few-layer graphene from the CVD-graphite/Ni surface using an optimized PDMS stamp.

Figure 2 Characteristics of the graphite/Ni sample grown via ACCVD. (a) Raman spectra of the graphite and mono-layer graphene (reference). The inset shows the SEM image of the graphite wrinkles (denoted by a blue arrow). (b) 3D laser scanning microscope image of the graphite/Ni surface. (c) Surface morphology magnified from the area highlighted by the dashed line and (d) the schematic illustration. The red and blue arrows indicate valley-like Ni grain boundaries and ridge-like graphite wrinkles, respectively.

Figure 3 Elasticity and flexibility of the PDMS plotted versus the PDMS cross-linking time. (a) Average elastic moduli and the standard deviations obtained from the six measurements that are summarized in Table 2. (b) Photograph of the deflections of the PDMS cantilevers under gravity, verifying that the flexibility is enhanced by reducing the PDMS cross-linking time.

Figure 4 PDMS adhesion and contactability with the graphite/Ni surface versus the PDMS cross-linking time. (a) Peel strength between the PDMS and the graphite/Ni surfaces. The inset shows a summary of average peel strengths and the standard deviations obtained from five measurements. (b) Microscope images of the optimal PDMS sample (cross-linking time of 25 min) and (c) a typical PDMS sample (cross-linking time of 60 min) debonded from the graphite/Ni substrate, and their corresponding schematic illustrations. Newly apparent patterns imprinted on the samples from the graphite/Ni surface are denoted by white arrows, implying improved contact with the optimal PDMS sample.

Figure 5 3D surface morphology of the optimal PDMS samples debonded from the graphite/Ni substrate. (a) 3D laser scanning microscope image of the optimal PDMS surface. (b) Magnified surface morphology of the area

highlighted with a dashed line and (c) the schematic illustration. The red and blue arrows denote ridge-like patterns imprinted from the Ni grain boundaries and valley-like patterns imprinted from the graphite wrinkles, respectively.

Figure 6 (a) Photograph of an array of graphite patterns as a graphene precursor. (b) AFM image of the patterned graphite (c) Microscope image of the directly and physically exfoliated few-layer graphene sheets on the PDMS surface.

Figure 7 (a) Raman spectra obtained from different few-layer graphene (including mono- and bi-layer graphene) patterns exfoliated on the PDMS surface. The arrow and asterisk highlight the peak at ~1410 cm^{-1} arising from δ CH_3 bend of the PDMS [19, 20, 25], verifying the existence of graphene on the PDMS surface. (b) Scanning Raman map showing I_{2D}/I_G obtained from the graphene sheets exfoliated on the PDMS surface. The scale bar indicates 5 μm.

Table 1

Processes	Parameters
Mixing ratio (monomer : curing agent)	10 : 1
Mixing	40 sec at 2000 rpm
Defoaming	20 sec at 2000 rpm
Degassing	20 min at -80 kPa
Cross-linking	20, 25, 30, 40, 60, 120 min at 70 °C

Table 2

	Cross-linking time (min)	Elastic modulus (kPa) Avg. ± S.D.	State	Handleability as a stamp
Insufficient cross-linking	0 ~ 20	N.A.	Liquid	N.A.
Partial cross-linking	20	10 ± 4	Sticky gel	Poor
	25	52 ± 6	Normal gel (Flexible & adherable)	Moderate
	30	420 ± 12	Very soft elastomer	Moderate
	40	1050 ± 20	Soft elastomer	Good
Typical cross-linking	60	1490 ± 40	Typical elastomer	Good
	120	1950 ± 90	Rigid elastomer	Good

Figure 1

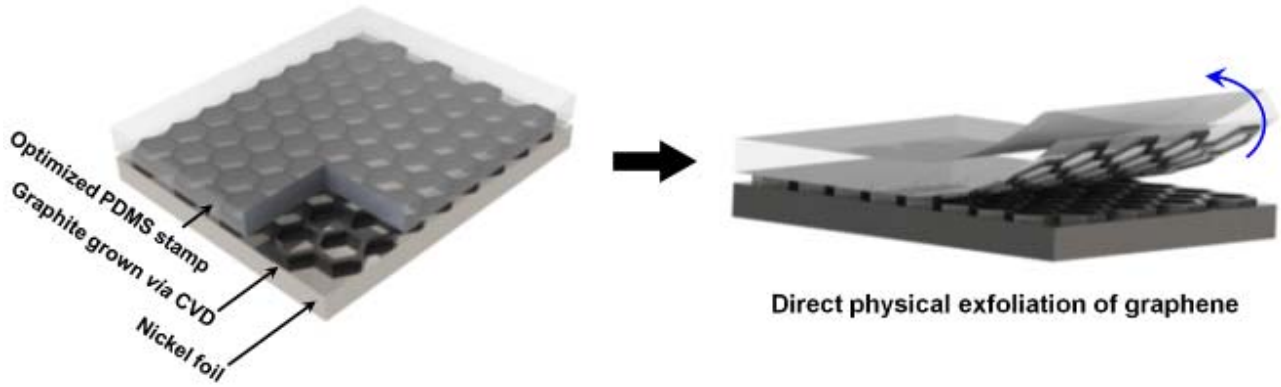
Optimized PDMS stamp
Graphite grown via CVD
Nickel foil
Direct physical exfoliation of graphene

Figure 2

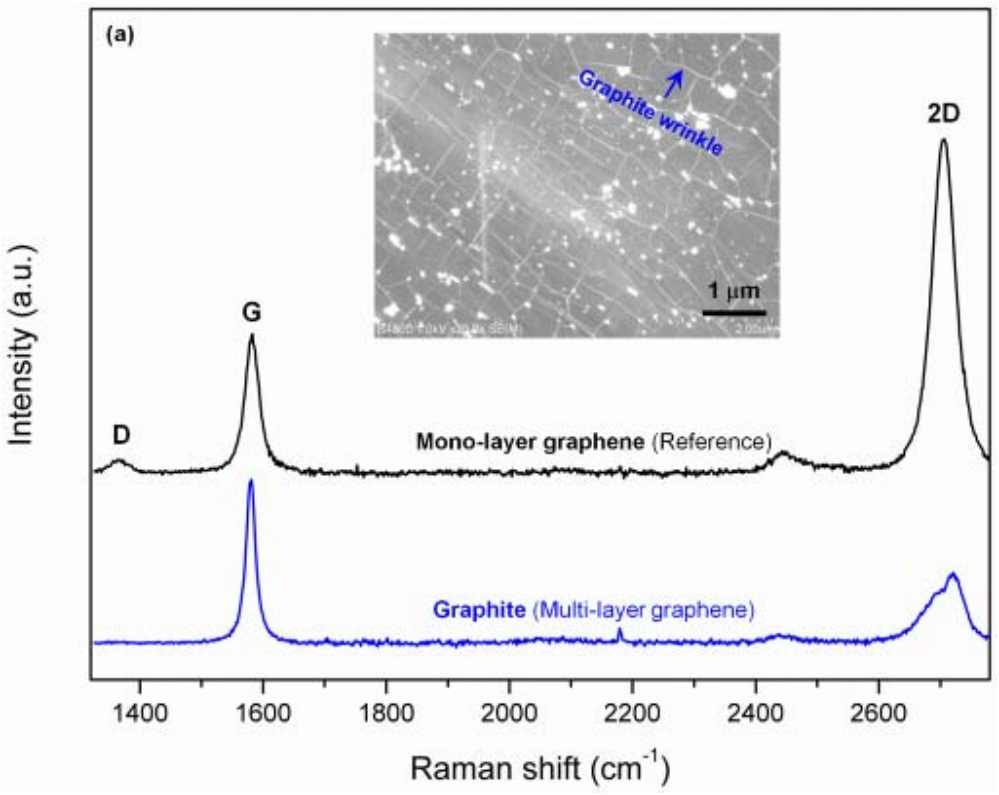
(a)
Graphite wrinkle
1 μm
2D
G
D
Mono-layer graphene (Reference)
Graphite (Multi-layer graphene)
Intensity (a.u.)
1400
1600
1800
2000
2200
2400
2600
Raman shift (cm-1)

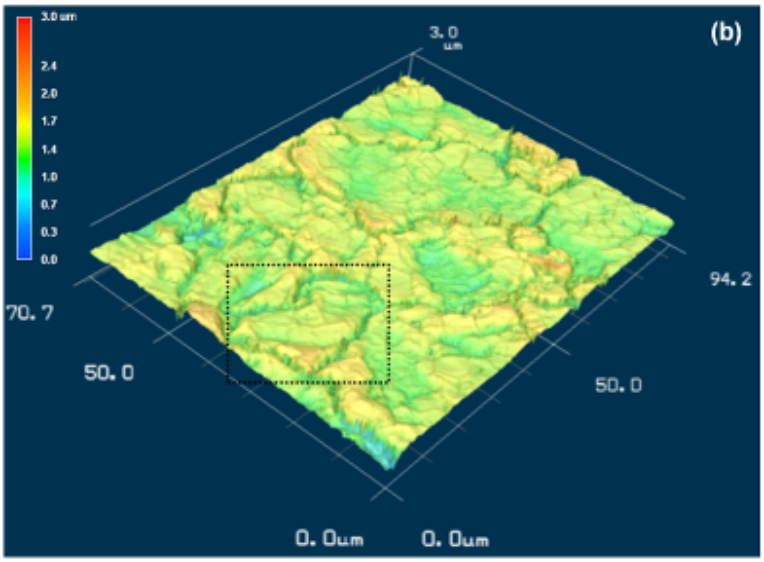
(b)
3.0 um
2.4
2.0
1.7
1.4
1.0
0.7
0.3
0.0
3.0 um
70.7
50.0
94.2
50.0
0.0um
0.0um

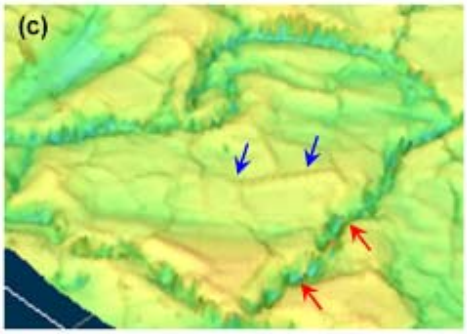
(c)

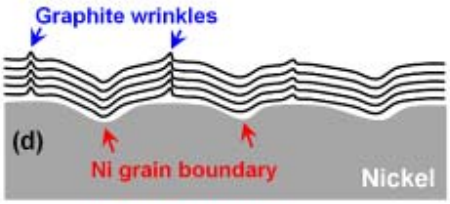
Graphite wrinkles
(d)
Ni grain boundary
Nickel

Figure 3

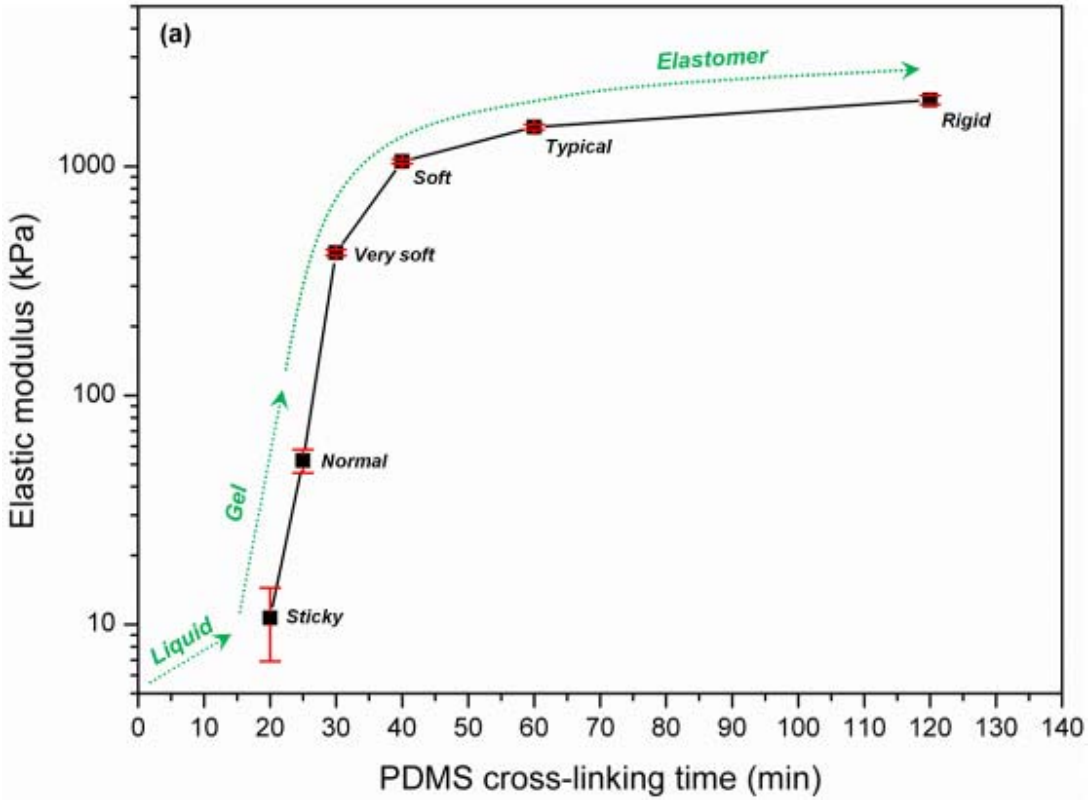
(a)
Elastomer
Rigid
Typical
Soft
Very soft
Normal
Sticky
Gel
Liquid
Elastic modulus (kPa)
1000
100
10
0
10
20
30
40
50
60
70
80
90
100
110
120
130
140
PDMS cross-linking time (min)

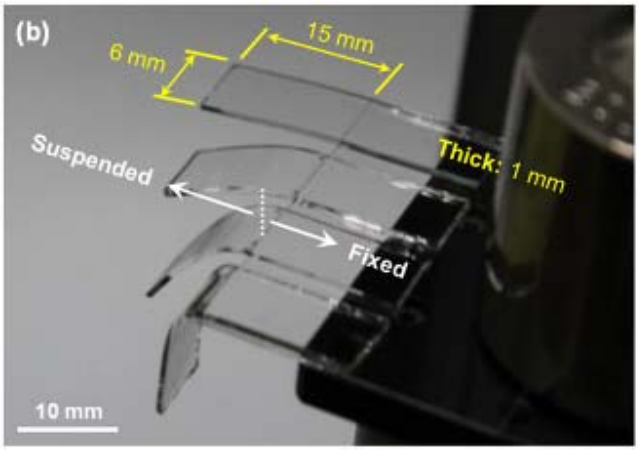
(b)
6 mm
15 mm
Suspended
Thick: 1 mm
Fixed
10 mm

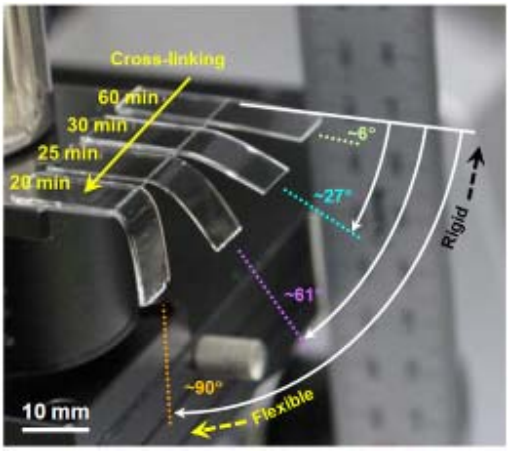
Cross-linking
60 min
30 min
25 min
20 min
~6°
~27°
~61°
~90°
Rigid
Flexible
10 mm

Figure 4

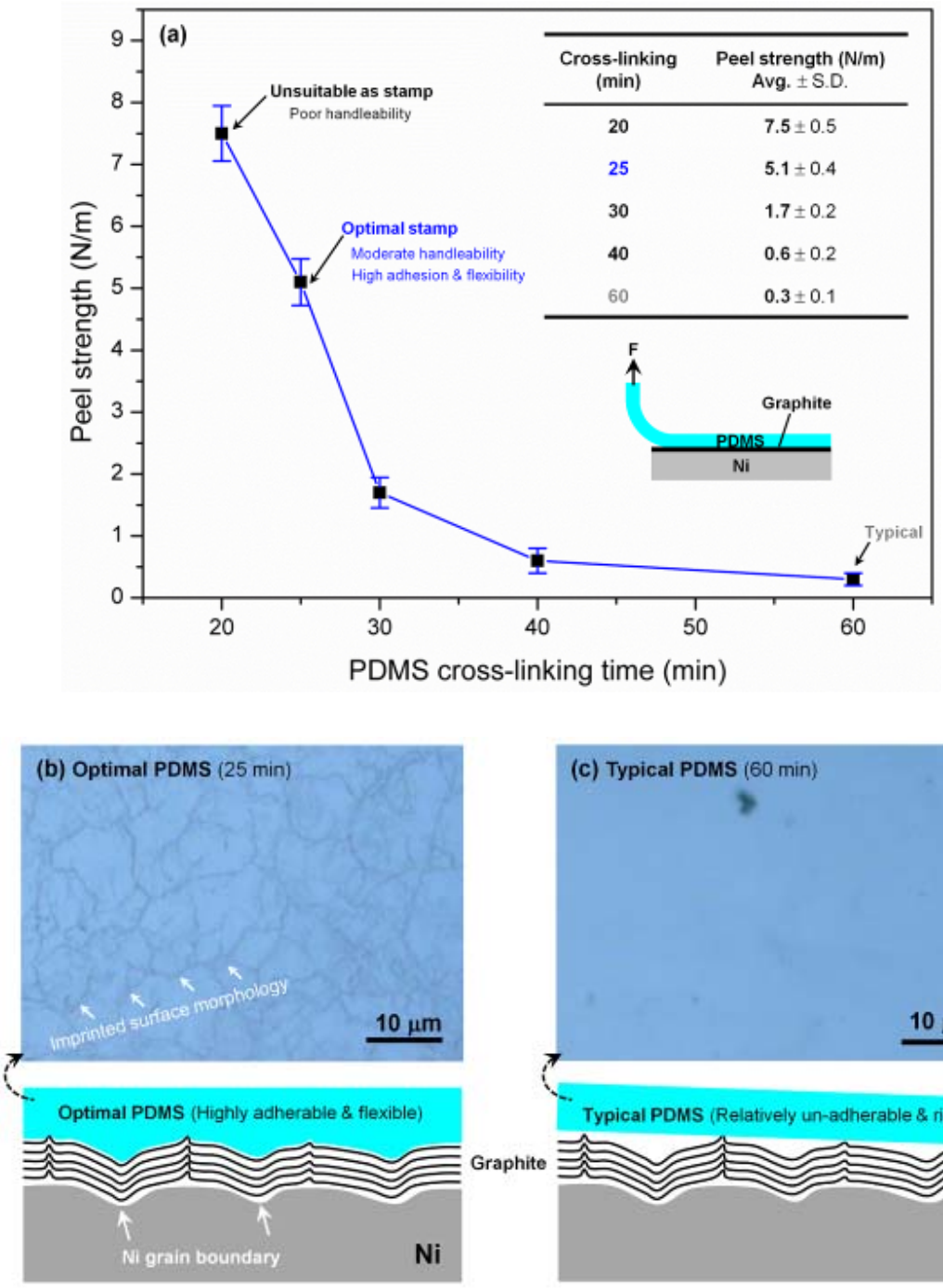
(a)
Peel strength (N/m)
PDMS cross-linking time (min)
Unsuitable as stamp
Poor handleability
Optimal stamp
Moderate handleability
High adhesion & flexibility
Typical
Cross-linking (min)
Peel strength (N/m) Avg. ± S.D.
20 7.5 ± 0.5
25 5.1 ± 0.4
30 1.7 ± 0.2
40 0.6 ± 0.2
60 0.3 ± 0.1
F
Graphite
PDMS
Ni
(b) Optimal PDMS (25 min)
Imprinted surface morphology
10 μm
Optimal PDMS (Highly adherable & flexible)
Ni grain boundary
Ni
Graphite
(c) Typical PDMS (60 min)
10 μm
Typical PDMS (Relatively un-adherable & rigid)

Figure 5

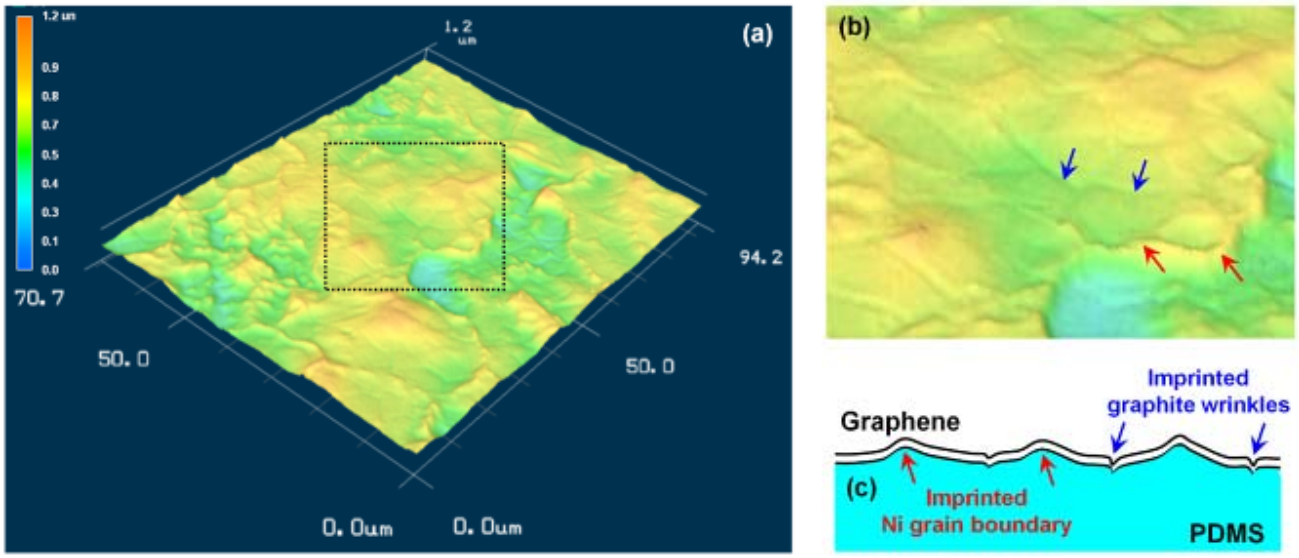
(a)
1.2 um
0.9
0.8
0.7
0.5
0.4
0.3
0.1
0.0
1.2
um
70.7
94.2
50.0
50.0
0.0um
0.0um
(b)
Graphene
Imprinted
graphite wrinkles
(c)
Imprinted
Ni grain boundary
PDMS

Figure 6

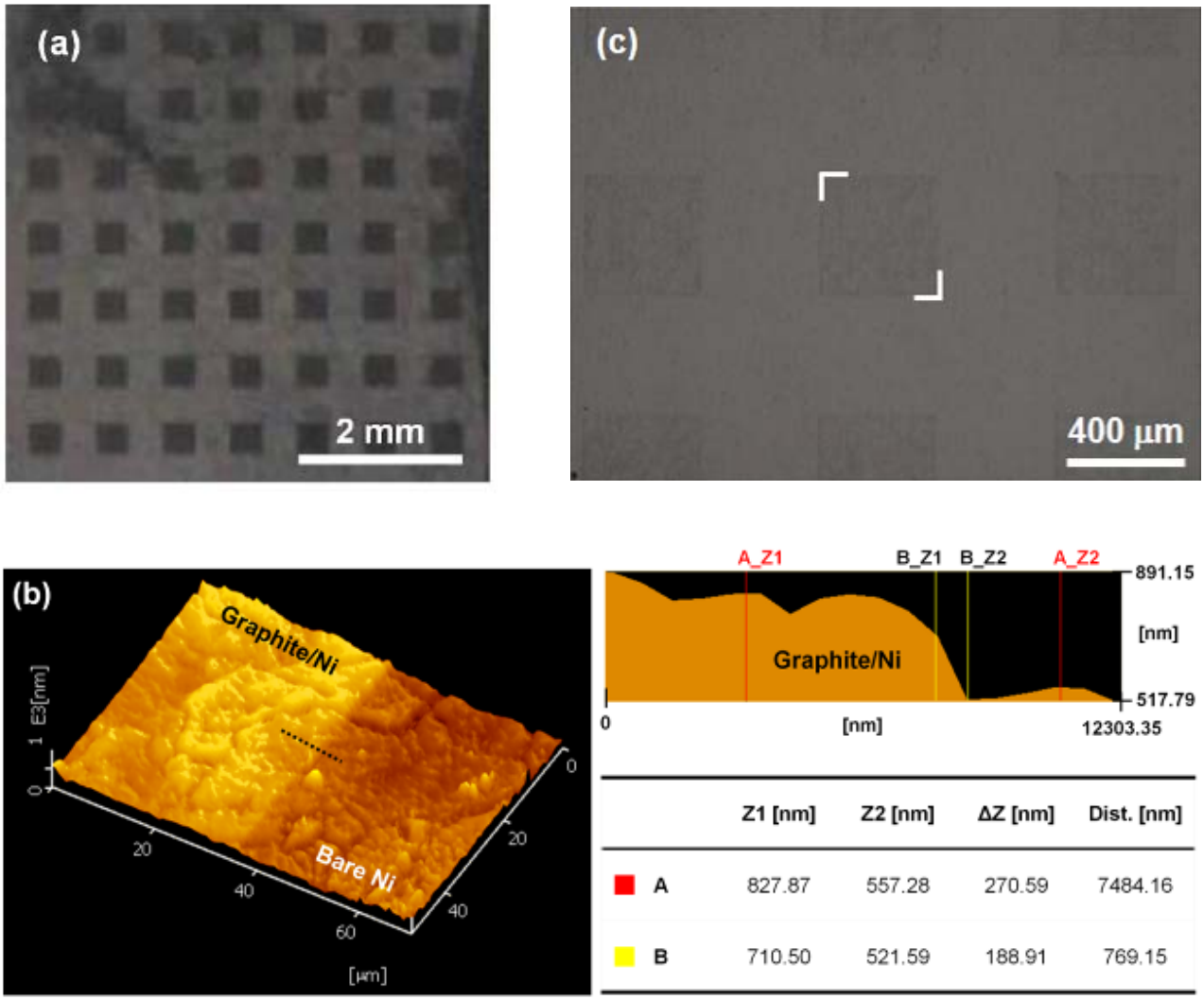

	Z1 [nm]	Z2 [nm]	ΔZ [nm]	Dist. [nm]
A	827.87	557.28	270.59	7484.16
B	710.50	521.59	188.91	769.15

Figure 7

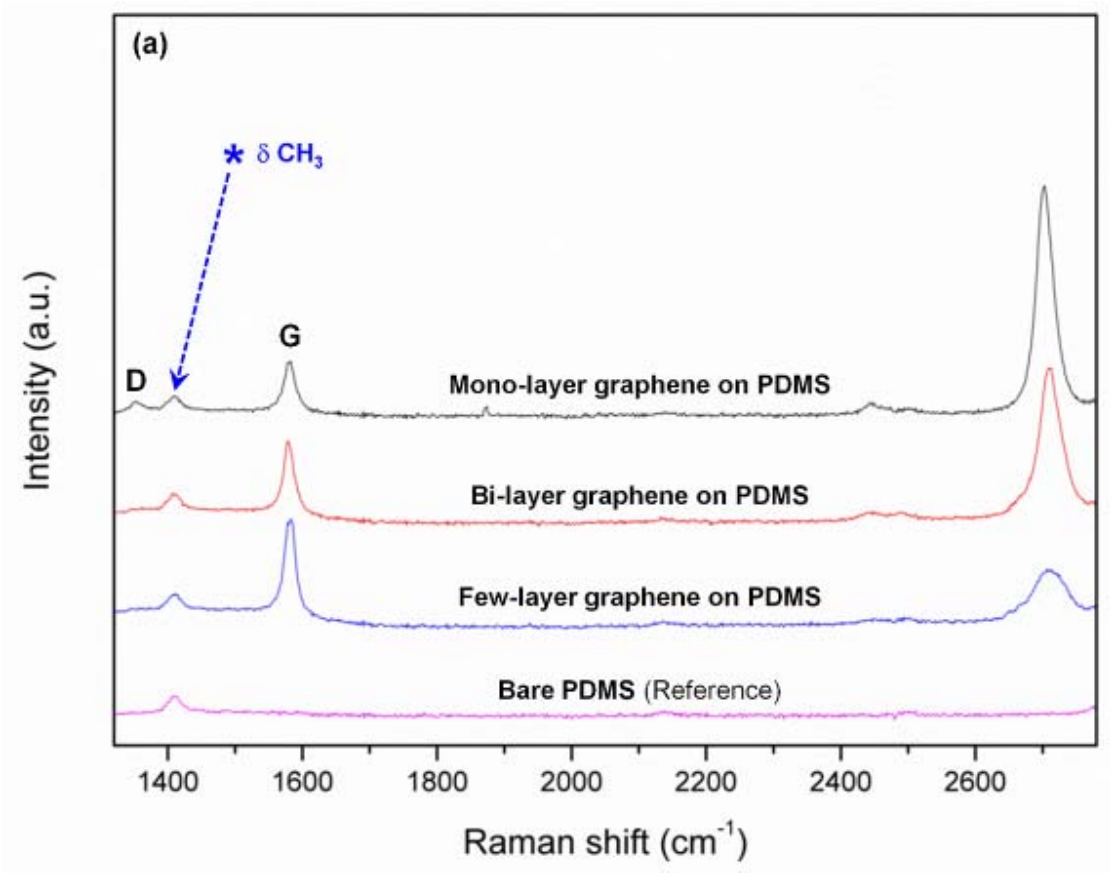
(a)
* δ CH3
D
G
Mono-layer graphene on PDMS
Bi-layer graphene on PDMS
Few-layer graphene on PDMS
Bare PDMS (Reference)
Intensity (a.u.)
1400
1600
1800
2000
2200
2400
2600
Raman shift (cm-1)

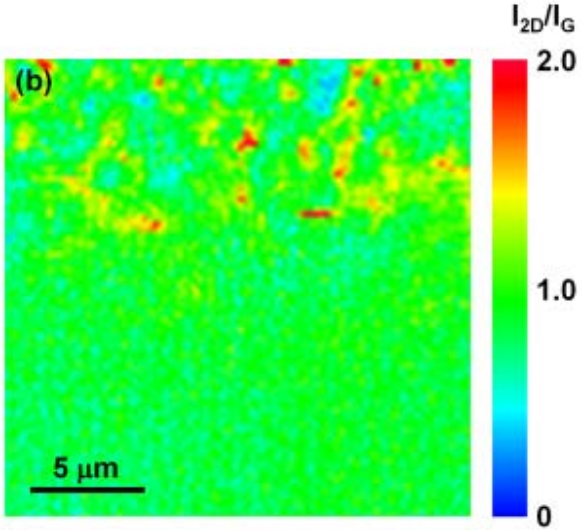
I2D/IG
2.0
1.0
0
(b)
5 μm